Journal of Environmental Radioactivity 205–206 (2019) 24–33

Contents lists available at ScienceDirect

Journal of Environmental Radioactivity

journal homepage: www.elsevier.com/locate/jenvrad

Dose calculations in aircrafts after Fukushima nuclear power plant accident – Preliminary study for aviation operations

A. Vargas[a,*], D. Arnold[b,c], M.-A. Duch[a], N. Evangeliou[d], K. Sievers[e], C. Maurer[b]

[a] Institute of Energy Technologies, Technical University of Catalonia, Barcelona, Spain
[b] ZAMG-Zentralanstalt für Meteorologie und Geodynamik, Vienna, Austria
[c] Arnold Scientific Consulting, ASC, Manresa, Spain
[d] NILU-Norwegian Institute for Air Research, Kjeller, Norway
[e] Klaus Sievers Aviation Weather, Lenggries, Germany

ARTICLE INFO

Keywords:
Dose estimates
Air traffic management
Monitoring
Regulation

ABSTRACT

There is little information to decision support in air traffic management in case of nuclear releases into the atmosphere. In this paper, the dose estimation due to both, external exposure (i.e. cloud immersion, deposition inside and outside the aircraft), and due to internal exposure (i.e, inhalation of radionuclides inside the aircraft) to passengers and crew is calculated for a worst-case emergency scenario. The doses are calculated for different radionuclides and activities. Calculations are mainly considered according to International Commission on Radiological Protection (ICRP) recommendations and Monte Carlo simulations. In addition, a discussion on potential detectors installed inside the aircraft for monitoring the aerosol concentration and the ambient dose equivalent rate, $H^*(10)$, for during-flight monitoring and early warning is provided together with the evaluation of a response of a generic detector. The results show that the probability that a catastrophic nuclear accident would produce significant radiological doses to the passengers and crew of an aircraft is very low. In the worst-case scenarios studied, the maximum estimated effective dose was about 1 mSv during take-off or landing operations, which is the recommended yearly threshold for the public. However, in order to follow the ALARA (As Low As Reasonably Achievable) criteria and to avoid aircraft contamination, the installation of radiological detectors is considered. This would, on one hand help the pilot or corresponding decision maker to decide about the potential change of the route and, on the other, allow for gathering of 4D data for future studies.

1. Introduction

The project European Natural Airborne Disaster Information and Coordination System for Aviation (EUNADICS-AV, 2016–2019, www.eunadics.eu) undertakes to develop and test a unique system to provide consistent and coherent information to aviation authorities, airlines and pilots in the event of a disaster affecting the airspace, including nuclear airborne emissions. EUNADICS-AV aims at bridging the gap between the data and the actual decision process. For natural disasters such as volcanic eruptions, there are regulations and guidelines, like those compiled on the website of EASA (https://www.easa.europa.eu/easa-and-you/safety-management/volcanic-ash) that assist the decision-making process, from air traffic management to the actual pilots. That is not the case in radiological emergencies, where significantly less guidance is available, like that compiled in the EASA Safety Information Bulletin SIB 2011–4 (EASA, 2011).

During events with release of nuclear material, like what happened in Fukushima, experience has shown that very little practical guidance is available to aviation and to pilots. The relevant ICAO (International Civil Aviation Organization) Annex 3, Meteorological Service for International Air Navigation (ICAO, 2016a), foresees the inclusion of a nuclear symbol in significant weather chart to indicate the location of the source, a text message which describes the extent of the cloud. In the future, when detailed information on the release is not available a radius of up to 30 km may be used, in addition to a vertical extent from the surface to the upper limit of the applicable airspace (ICAO, 2016b).

Evaluation of a crisis management exercise conducted by Eurocontrol in 2014 resulted in a long list of items required to better prepare for the future, most prominent being the issuance of charts that show the spread of radioactivity in the air at commonly used flight altitudes. At present, no such charts are available to air traffic control, airlines or pilots (ICAO, 2016b).

In case of a radiological emergency, for example as a result of a severe nuclear power plant accident or a nuclear weapon detonation,

* Corresponding author.
E-mail address: arturo.vargas@upc.edu (A. Vargas).

https://doi.org/10.1016/j.jenvrad.2019.04.013
Received 6 September 2018; Received in revised form 23 April 2019; Accepted 26 April 2019
Available online 13 May 2019

with a significant release into the atmosphere, en-route flights or taking-off/landing aircrafts can encounter the emitted radioactive cloud and fly through it without noticing it, as there are no radiation detectors on commercial aircrafts. This could pose a health risk to both passengers and crew. In such an event, the exposure pathways can be either through cloud- and ground-shine from external gamma photons or directly by internal contamination through inhalation. From an operations perspective, the doses can be calculated in two different flight situations: the aircraft is outside the cloud or the aircraft is inside the cloud. In the first case, the contribution to the dose is only due to the external exposure due to the photons from the radioactive cloud that will deposit energy into individuals in the aircraft. If, on the contrary, the aircraft is inside the cloud or passes through it, the dose contributions will be due to: a) external dose from the cloud outside and inside the aircraft, b) external dose from deposited radioactive particles in both outside and inside the aircraft surfaces, and c) internal doses due to inhalation of the radioactive aerosol. The ingestion pathway is neglected in both situations.

Besides the radiological risk to the human beings in the vessel, an aircraft intersecting a radioactive cloud will become contaminated and a decontamination process, under a regulated procedure, should therefore follow after landing preventing the aircraft to be used until it is declared as “non-radiologically contaminated”. Although the economic impact of such a contamination may be significant or even critical for some small flight companies, it is not within the scope of this paper to make an economic assessment.

In addition to making a first assessment of the doses that could be reached either based on uncertain forecasts or after-flight, a preventive or early-warning approach could be taken by introducing radiological monitoring devices into the planes so that the basic criteria in radiological protection of “as low as reasonable achievable” (ALARA) could be achieved based on decisions on the fly. An initial step of understanding the response of detectors to measure the radiological risk is therefore needed and addressed in this work. It is worth noting that such detectors could as well provide, not only the radiological dose but also potentially distinguish whether the aircraft is inside the cloud or if it is approaching to the cloud and thus allow for a rerouting possibility. Finally, unlike in other types of hazards, there is a general lack of measurement data for radionuclide emissions in upper layers of the atmosphere since automatic and non-automatic systems are located at ground level, where the population resides. Having monitors installed in aircrafts would provide crucial information to develop further any guidelines or recommendations to support pilots to take decisions.

2. Methodology

2.1. Radionuclides selection

A large number of radionuclides are present in case of a radiological accident in a nuclear power plant or after a nuclear explosion. In order to constrain the radionuclides to a feasible number, a dose-based approach is taken. In this approach, the radionuclides selected were the most contributing to the internal and external dose in case of a NPP accident such as Fukushima and Chernobyl (this value is corroborated by internal EUNADICS-AV studies performed by the Radiation and Nuclear Safety Authority of Finland, STUK). Table 1 shows the list of radionuclides used in the follow-up dose calculations and their main radioactive characteristics.

2.2. Calculation of activity concentration inside the aircraft and activity deposited on the vessel walls

The temporal evolution of the volumetric activity inside the aircraft can be calculated with the following equation (Eq. (1)):

$$\frac{dC_i(t)}{dt} = \frac{Q_{fresh}(1-\varepsilon_{fresh})}{V}C_o(t) + \lambda C_{i-1}(t) - \left(\lambda + \frac{Q_{rec}\varepsilon_{rec}}{V} + X_d + \frac{Q_{fresh}}{V}\right)C_i(t) \quad [1]$$

where.

C_i is the volumetric activity of radionuclide i inside the aircraft in Bq m^{-3}, C_o is the volumetric activity of radionuclide i outside the aircraft in Bq m^{-3}, Q_{fresh} is the air renewal flow rate of the aircraft (fresh air) in $m^3\,h^{-1}$, Q_{rec} is the air recirculation flow rate of the aircraft in $m^3\,h^{-1}$, V is the volume of the aircraft in m^3, λ is the decay constant of the radionuclide in h^{-1}, X_d is the deposition rate of the radionuclide particles in h^{-1}, ε_{fresh} is the efficiency of the entrance filter, i.e, for the fresh air, and ε_{rec} is the efficiency of the recirculation filter.

To estimate the internal dose (i.e. due to inhalation), only the relevant sub-set of the selected radionuclides is used. This includes ^{134}Cs, ^{137}Cs, ^{131}I, ^{132}Te and ^{132}I. For ^{134}Cs, ^{137}Cs, ^{131}I and ^{132}Te the activities of the progenitor concentration are zero, $C_{i-1} = 0$. In addition, ^{132}I activity is considered to be in equilibrium with ^{132}Te.

Air renewal and filtering is of course a crucial aspect. The European Aviation Safety Agency (EASA) indicates that each passenger and crew compartment must be ventilated with enough fresh air but not less than $0.3\,m^3\,min^{-1}$ STP (Standard Temperature and Pressure. This renewal is achieved through circulation inside the cabin (Fig. 1) until eventually the air is drawn into the lower fuselage, where approximately half of it is vented overboard through a pressurization outflow valve. The remaining portion is remixed with a fresh supply from the engines and run through High Efficiency Particulate Air (HEPA) filters. Then the cycle begins again.

As example, with a minimal renewal of 5 L/s per person in an Airbus A320-200 and 160 passengers on board the plane with a cabin volume of $330\,m^3$, leads to an air renewal of 2.5 min.

According to Fig. 1, ε_{fres} is set to 0 since there is no filter for the fresh air but only for the recirculating air. The value for ε_{rec} for HEPA filter is about 99% for particulate matter. It should be taken into consideration that, for noble gases and Iodine in gaseous form, the retention efficiency of the HEPA filter would only be granted if an activated carbon filter was included. However, the authors have not found enough information on the response of HEPA filters without the carbon filter to those species and therefore a conservative approach has been assumed, whereby there is no retention for them. For noble gases, the internal dose is not significant and only external dose has to be considered. However, for ^{131}I in gas form, internal dose is important being ^{131}I one of the most significant radionuclides. Given that we aim at taking a conservative approach, and to ensure we lean towards the worst-case scenario, also retention efficiency is set to zero for particulate matter.

Constant values of the radioactive cloud concentration, C_o, have been chosen for solving the concentration equation (1) inside the aircraft.

In order to estimate the deposition of aerosol particles onto the inside surfaces of the aircraft, the deposition rate, X_d, should be calculated. For indoors, assuming a surface roughness similar to that of a filter paper, the frictions velocities, u^*, are between 20 and $60\,m\,h^{-1}$(Ahmed, 1979). According to different studies (e.g. Porstendörfer, 1994) the deposition velocities normalized by the friction velocity (u^*) can be obtained from the relationship with the particle diameter. For example, a value of $4{\cdot}10^{-4}$ for the ratio v_g/u^* is obtained for an activity size diameter close to 1 μm and a surface roughness similar to that of a filter paper. Therefore, an average deposition velocity of about 0.02 m h^{-1} can be derived using $u^* = 40\,m\,h^{-1}$. Considering a large surface volume ratio in the aircraft of about $10\,m^{-1}$, the average deposition rate, X_d, is then $0.2\,h^{-1}$.

Taking the Airbus A320-200 as a generic aircraft with its dimensions, the pressurized fuselage volume is about $330\,m^3$. For a unit radionuclide concentration in the radioactive cloud, and using the

Table 1
List of radionuclides in an emergency radiological scenario and their main characteristics.

Radionuclide	$T_{1/2}$	Decay mode, energy (max, average for beta) in keV (probability*100)
^{137}Cs	30.05 years	β^-: 514–174(94.36); 1176–416(5.64) γ: 661.7(85)
^{134}Cs	2.064 years	β^-: 89.06–23.2(27.27); 415.64–123.6(2.5); 658.39–210.3(70.19) γ: 475.4(1.5); 563.25(8.34); 569.33(15.4); 604.72(97.63); 795.86(85.47); 801.85(8.694); 1038.65(0.99); 1168(1.791); 1365.19(3.019)
^{131}I	8.0233 days	β^-: 247.9–69.35(2.13); 333.8–96.61(7.20); 606.3–191.59(89.4) γ: 80.2(2.607); 284.305(6.14); 364.489(81.2); 636.989(7.12); 722.911(1.786)
^{132}Te decays to ^{132}I	3.230 days	β^-: 240–67.0(100) γ: 49.72(15.1); 111.81(1.85); 116.34(1.97); 228.327(88.12)
^{132}I	2.295 h	β^-: 742–242.7(13.0); 1186–422.1(19.0); 1618–608.1(12.3); 2141–841.8(19.0) γ: 505.79(4.93); 522.65(16.0); 630.19(13.3); 667.714(98.7); 669.8(4.6); 671.4(3.5); 772.6(75.6); 812.0(5.5); 954.6(17.6); 1398.57(7.01)
^{88}Kr	2.825 h	Produced by ^{235}U(n,F). Therefore, most of the activity will decay before it reaches the aerial space. β^-: 526–137.3(67); 686–228.5(9.1); 2919–1235.4(14) γ:196.3(26.0); 834.83(13); 1529.77(10.9); 2195.84(13.2); 2392.11(34.6)
^{133}Xe	5.2474 days	β^-: 346.4–100.6(99.12) γ: 81(37.0)
^{135}Xe	9.14 h	β^-: 915–320.2(96) γ: 249.8 (90)

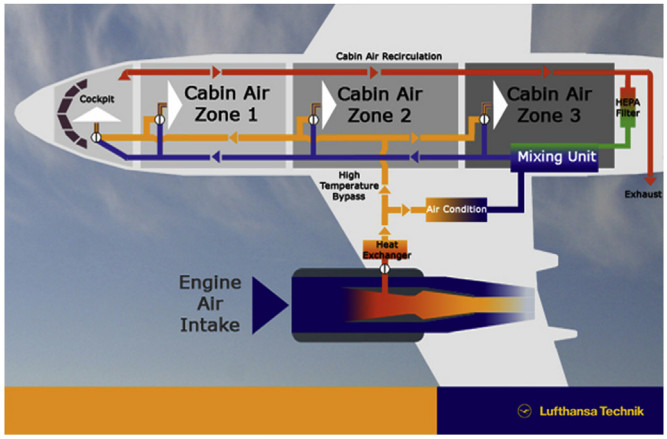

Fig. 1. Airflow inside a generic aircraft cabin (Lufthansa technical report, https://www.lufthansa-technik.com.).

aircraft characteristics, deposition and all the parameters as described above to solve to Equation (1), the temporal evolution of the concentration inside the cabin reaches a stable value of about the half of the outside concentration in a short period of time of less than 10 min. However, in a rough approximation and considering a cruise altitude between 9 and 11 km a.s.l., it is considered that the air density inside the cabin is approximately double than outside density, thus both will have almost the same concentration per unit volume.

2.3. Calculation of the internal dose – Committed dose per unit intake (DPUI)

The internal effective dose, E in mSv, for a radionuclide i with a concentration C_i (Bq m^{-3}) inside the aircraft cabin for a time period exposure of t hours and breathing rate of $\dot{V}$ (m^3 h^{-1}) will be calculated using the following equation:

$$E = DPUI_i \cdot C_i \cdot \dot{V} \cdot t \quad [2]$$

Provided that the concentration and the period that the passengers are exposed to such concentrations and the breathing rate are known, the committed dose per unit intake (DPUI in mSv per Bq) is used to estimate the effective dose as a function of the cloud concentration in equation (2). DPUI values were obtained from ICRP publication 71 (ICRP, 1995). Recommended values in ICRP 71 of absorption into blood and an activity mean aerodynamic diameter (AMAD) of 1 μm has been considered. For the selected radionuclides, rounding DPUI for a 3-months baby has been selected for conservative dose calculations since for adults DPUI values are lower than for babies. In Table 2, DPUI values used for dose calculations are shown.

Table 2
Committed effective doses per unit Bq intake in mSv Bq^{-1} for different radionuclides and forms.

Radionuclide	DPUI (mSv per Bq)
^{131}I particle	7.00E-05
^{131}I gas	1.50E-04
^{134}Cs	1.20E-05
^{137}Cs	1.00E-05
^{132}Te + ^{132}I	5.00E-05

In the case of Tellurium, its chemical form can be both in gas and vapor as well as in particulate aerosol. There is scarce information about the behavior of tellurium in an accidental release. Therefore, its daughter, the ^{132}I, has been considered for the dose evaluation using its corresponding systemic biokinetics. In this way, the DPUI for ^{132}Te in equilibrium with ^{132}I has been considered and the gas form was chosen in order to be conservative in the dose calculations.

2.4. Calculations of H*(10)

The ambient dose equivalent rate, $\dot{H}^*$ (10), in μSv/s is calculated using the following equation:

$$\dot{H}^*(10) = k_o \gamma A \sum_{i=1}^{n} \phi_i E_i \left(\frac{\mu_{en}}{\rho}\right)_i F_i \quad [3]$$

where.

k_o is the conversion unit coefficient 1.602 10^{-4} μGy per MeV g^{-1},
γ is the yield for the corresponding gamma decay of the radionuclide in s^{-1} Bq^{-1}, A is the activity in Bq,
ϕ_i is the fluence per incident photon of energy i expressed in cm^{-2},
E_i is the energy of the incident photon in MeV, (
$\mu_{en}/\rho)_i$ is the mass energy transfer coefficient for energy i in cm^2/g obtained from the NIST Standard Reference Database (Hubbell, JH. and Seltzer, 2004), and
F_i is the conversion coefficient from air-kerma into ambient dose equivalent for energy bin i (ISO 4037-3, 1999) in μSv/μGy.

The fluence energy distribution ϕ_i for a pre-defined geometry is calculated using the Monte Carlo code PENELOPE/PenEasy (Sempau et al., 2011). PENELOPE (Salvat et al., 2011) is a code for the coupled electron-photon transport in arbitrary materials in a wide energy range,

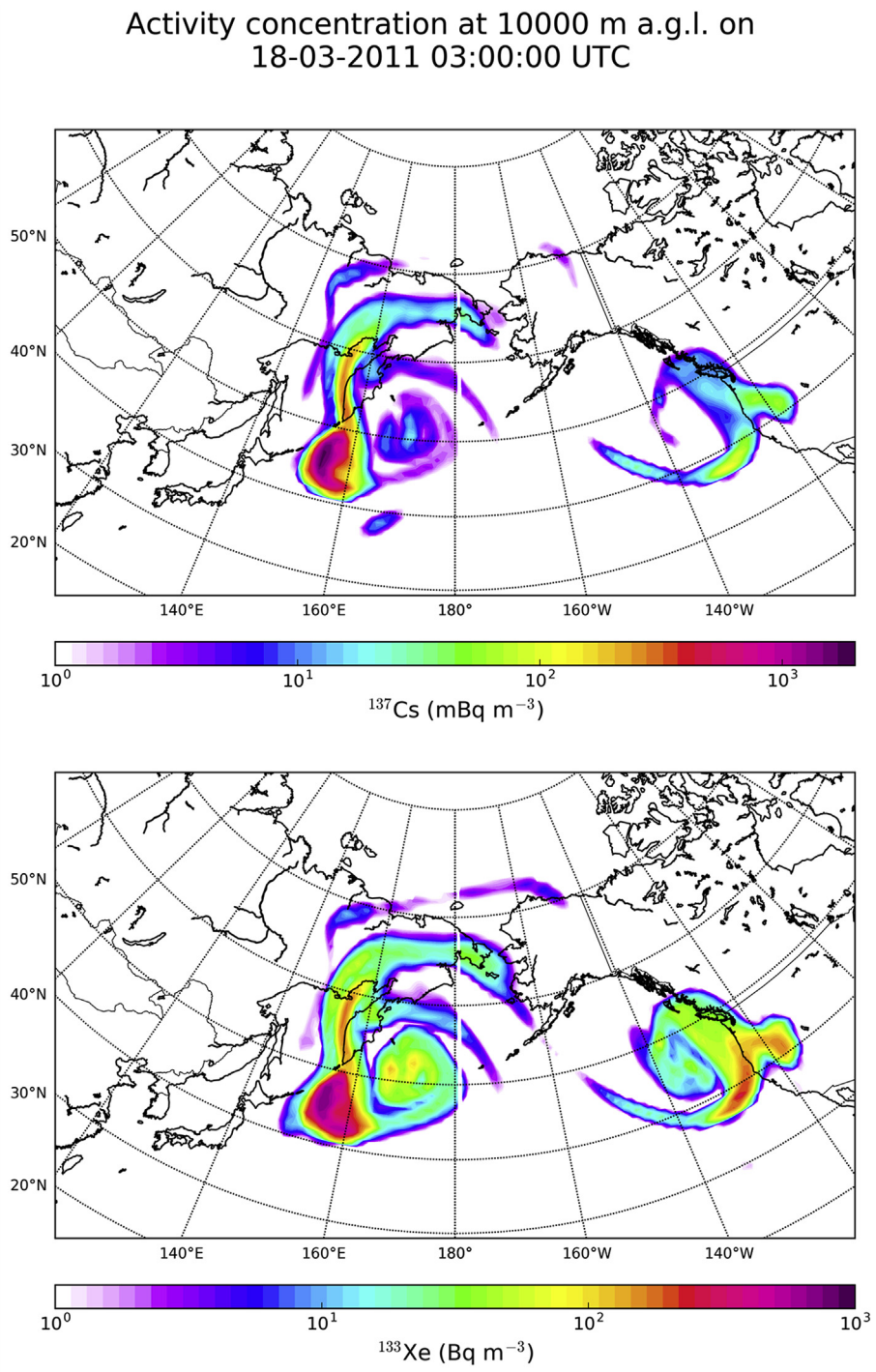

Fig. 2. ^{133}Xe (left) and ^{137}Cs (right) concentrations at 10.000 m height on 18th March 2011 at 03h00 UTC.

spanning from a few hundred eV to about 1 GeV. The core of the program is a set of Fortran subroutines. In this work, penEasy has been adopted as the steering main program, which includes a set of source models, tallies and variance-reduction techniques.

With PENELOPE/penEasy, the fluence is calculated for different source geometries: i) gamma decays from radionuclides in a radioactive cloud, ii) gamma decays from deposited particles on the outside walls of the aircraft and iii) gamma decays from deposited particles on the inside walls of the aircraft.

Two main scenarios have been used to estimate the spectrum response of a spectrometric detector installed inside the aircraft: a) the aircraft is outside the cloud and b) the aircraft is inside the cloud.

The geometry used to calculate the fluence energy distribution inside the aircraft has been simplified assuming that there is no attenuation from the walls of the aircraft. This assumption overestimates the dose and is used in order to calculate the doses for the worst-case scenarios that are described in the next sections. This is in line with the conservative approach taken in the paper.

2.5. Scenario preparation: atmospheric transport modeling for a nuclear power plant accident

In order to perform the calculations of the estimated doses, a scenario or a set of scenarios need to be defined. To this aim, the

Table 3
Calculated time integrated concentrations according to ^{133}Xe concentrations obtained from Fig. 2.

Concentration (Bq m^{-3})	Time exposure (h)	Time integrated concentration (Bq m^{-3} h)
700	0.083	58
500	0.167	83
100	0.25	25
50	0.5	25
10	2	20
5	3	15
1	4	4
TOTAL	10	185

Table 4
Time integrated concentration for each radionuclide and average concentration for transoceanic flight during Fukushima accident in a worst-case scenario.

Radionuclide	Time integrated concentration (Bq m^{-3} h)	Average concentration (Bq m^{-3})
^{131}I particle	1.85E+00	1.85E-01
^{131}I gas	3.70E+00	3.70E-01
^{134}Cs	1.85E-01	1.85E-02
^{137}Cs	1.85E-01	1.85E-02
^{132}Te+^{132}I	4.63E-02	4.63E-03
^{88}Kr	1.85E+00	1.85E-01
^{133}Xe	1.85E+02	1.85E+01
^{135}Xe	1.85E+00	1.85E-01

Lagrangian particle dispersion model FLEXPART (Stohl et al., 2005) version 10 was used to simulate transport of radionuclides emitted from the Fukushima Dai-ichi nuclear power plant (NPP) accident and obtain the 4D concentration fields of selected radionuclides. FLEXPART was forced by European Center for Medium-Range Weather Forecasts (ECMWF) operational meteorological analyses from the Integrated Forecast System (IFS) with 137 model levels and a horizontal resolution of 0.5° × 0.5°.

Emissions were adopted from Stohl et al. (2012) for ^{137}Cs and ^{133}Xe for the period between 10 March 2011 at 12.00 and 20 April 2011 at midnight following 3-hourly intervals (932 releases in total) over three altitudes (0–50 m, 50–300 m and 300–1000 m). The model ran forward in time emitting 300,000 particles per release, giving a total of about 279.6 million particles. The tracers ^{137}Cs and ^{133}Xe were used in the FLEXPART set-up. It is also good to highlight that this source term is known to be overestimating the source term, which is advantageous for this study as it focuses on the worst-case scenario approach.

While xenon is a noble gas and it is not subject to scavenging processes, caesium is almost entirely attached onto particle surfaces. Therefore, the simulations for ^{137}Cs accounted for wet and dry deposition (Stohl et al., 2012), assuming a mean particle diameter of 0.4 μm used commonly for such simulations and a density of 1900 kg m^{-3} (Krinstiansen et al., 2016). The wet deposition scheme considers below-cloud and in-cloud scavenging separately based on cloud liquid water and cloud ice content, precipitation rate and cloud depth from ECMWF, as described in Grythe et al. (2017). The dry deposition scheme in FLEXPART is based on the resistance analogy (Slinn, 1982).

2.5.1. Worst-case scenarios in case of a NPP accident: Fukushima

Two scenarios have been defined for the Fukushima NPP accident in order to evaluate the radiological dose: i) *Fictitious Cruise scenario* - at cruising speed and altitude. In this case a transoceanic flight over the Pacific Ocean during the Fukushima accident has been evaluated and ii) *Fictitious Take-off/landing scenario* - low altitude flight when the aircraft is in the taking off or landing operations. In this case, the aircraft is located close to the Fukushima NPP, i.e., when and where concentrations levels were extremely high.

2.5.1.1. Fictitious Cruise scenario - Transoceanic flight during Fukushima accident. For this scenario it was assumed that within travel time, 10 h, the flight encounters the radioactive cloud. The concentrations for ^{137}Cs and ^{133}Xe were estimated from the simulation at a height of 10 km above ground level. Although this does not correspond exactly to the corresponding 300 hPa flight level, it comes close enough to perform the study without having to do the conversion to flight levels.

The simulation (Fig. 2) shows that the concentration of ^{137}Cs is about three orders of magnitude lower than that of ^{133}Xe at this height. Given that the simulation has only been made for ^{137}Cs and ^{133}Xe, a way to infer the concentrations of the remaining significant radionuclides is required. Based on the paper of Masson et al. (2011), the following assumptions have been made: i) ^{134}Cs concentration is similar to ^{137}Cs, ii) The concentration of ^{131}I in particle form is about 10 times higher than that of ^{137}Cs iii) The ratio of particulate to gas form for ^{131}I is approximately 0.5, and iv) The ratio of ^{132}Te concentration to ^{131}I in particle form is close to 2.5%.

^{88}Kr and ^{135}Xe decay very quickly and will not reach the atmosphere in huge quantities for this scenario, therefore a concentration of two orders of magnitude lower than ^{133}Xe was assumed for the dose calculations. This is in line with the work by IRSN (IRSN, 2011) on the evaluation of the emissions till 22nd of March.

Based on the atmospheric transport simulations, a time period where concentrations were high at high altitudes was selected to make a conservative estimate of the integrated concentrations. No realistic flight tracks have been used. The portions of the time that the aircraft is flying inside the radioactive cloud with specific 133Xe concentrations using the selected simulation snapshot are summarized in Table 3, together with the corresponding time integrated concentration. It is important to note that, within the EUNADICS-AV project, dose estimates, based on derived source terms and atmospheric transport calculations will be available on realistic flight tracks. Table 4 shows the time integrated concentrations for each radionuclide and the average concentrations during the 10-h flight.

2.5.1.2. Fictitious Take-off/landing scenario - Low altitude flight. In this scenario, it was assumed that the aircraft is flying close to the ground level over a period of 30 min and within an area with radius 100 km centered in the NPP, in order to consider the landing and taking off operations close to the accident. The assumption of 30 min for landing and taking off operations is extremely conservative, even more, considering that in an emergency situation as described, these operations would be reduced to minimum time and probably will take only a few minutes.

The radionuclide concentrations in this scenario have been obtained based on the literature on the analysis of time series measurements carried out close to the Fukushima NPP at ground level and simulations using the FLEXPART model at 500 m a.g.l.

The estimated release rates time-series of radionuclides from the Fukushima NPP just after the accident are largely uncertain, because only radiation dose rates and/or very limited data of atmospheric radionuclides are available. In addition, atmospheric radionuclide concentrations simulated by atmospheric transport models with an estimated source term have also large uncertainty, due to uncertainties in the involved meteorological input data and the dispersion model itself and above all they cannot be validated due to the lack of observational data. Although the observed deposition densities of radionuclides on the ground were used to estimate internal radiation doses in some cases, the time integrated atmospheric radionuclide concentrations for quantifying inhalation derived from these estimates have yet again large uncertainties. Therefore, in the work of Hirayama et al. (2015), the temporal evolution of the ^{131}I concentration was estimated using measured spectra from NaI(Tl) detectors. In this work, which has been

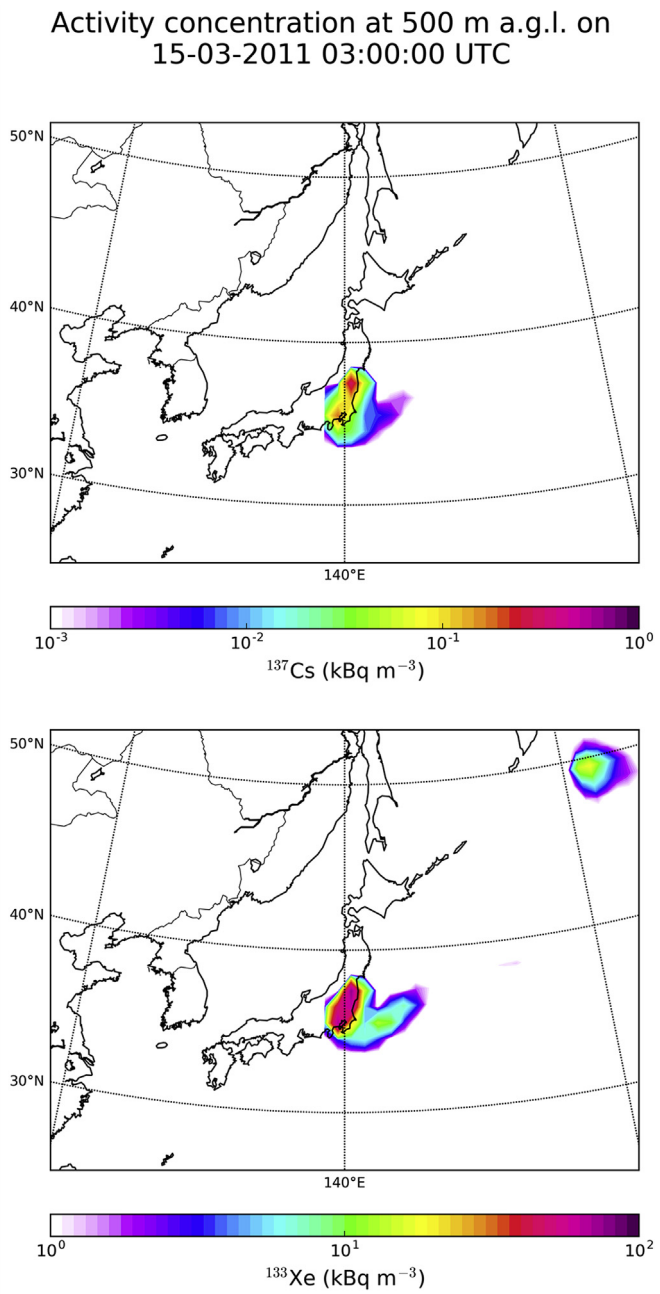

Fig. 3. ^{133}Xe and ^{137}Cs concentrations at 500 m height on 15th march 2011 at 03h00 UTC.

used as a reference, the location of 13 measurement stations in the cities of Futuba, Okuma, Naraha, Tomioka, Hirono and Fukushima, their time integrated and average ^{131}I were estimated. According to data obtained from this work (Hiramaya et al., 2015), an average ^{131}I concentration in gas form of 10 kBq m^{-3} has been chosen for a flight time of half an hour during the landing or taking off operations. The ratio of ^{131}I particulate to ^{131}I gas is the same as for transoceanic flight, i.e., 0.5, given an average ^{131}I concentration in particulate form of 5 kBq m^{-3}.

In Fig. 3 simulations of the concentrations of ^{133}Xe and ^{137}Cs at 500 m altitude are shown just after the accident. A ratio of about 200 is estimated, which is lower than for the transoceanic flight due to the deposition of ^{137}Cs. From the simulation 100 kBq m^{-3} and 500 Bq m^{-3} for ^{133}Xe and ^{137}Cs respectively have been chosen for a flight time of half an hour during the landing or taking off operations. The ratios of ^{133}Xe to ^{137}Cs and ^{137}Cs–^{134}Cs are the same as for transoceanic flight.

Table 5
Time integrated concentration for each radionuclide and average concentration for low altitude flight close to Fukushima just after the accident.

Radionuclide	Time integrated concentration(Bq m^{-3} h)	Average concentration(Bq m^{-3})
^{131}I particle	2.50E+03	5.00E+03
^{131}I gas	5.00E+03	1.00E+04
^{134}Cs	2.50E+02	5.00E+02
^{137}Cs	2.50E+02	5.00E+02
^{132}Te+^{132}I	2.50E+03	5.00E+03
^{88}Kr	5.00E+03	1.00E+04
^{133}Xe	5.00E+04	1.00E+05
^{135}Xe	5.00E+03	1.00E+04

The UNSCEAR 2013 report (UNSCEAR, 2013) has been used to estimate the ratio of ^{132}Te to ^{137}Cs concentrations in air. At the start of the emission, the ratio of ^{132}Te to ^{137}Cs was around 10, which drastically decrease after a few days due to the different decay half-life.

For ^{88}Kr and ^{135}Xe concentrations, due to their short lives, most of these radionuclides will decay before it reaches the aerial space. However, it has been anyway included with a concentration 10 times lower than ^{133}Xe (IRSN, 2011).

Table 5 shows the time integrated concentrations for a half hour flight and the average concentrations that are used for dose calculations.

3. Results and discussion

3.1. Effective dose estimation due to radionuclide inhalation

3.1.1. Fictitious cruising speed and altitude. Transoceanic flight during Fukushima accident at cruising speed and altitude

A breathing rate of 1 m3 h-1 for passengers and crew is assumed according to the ICRP (ICRP, 1994) recommended values for resting and light exercise. Table 6 shows the committed effective dose for this worst-case scenario using approximately values of DPUI coefficients given for a 3-month old baby.

3.1.2. Fictitious Take-off/landing scenario - Low altitude flight

Table 6 shows the committed effective dose for the worst-case scenario. A total dose of 1.1 mSv has been estimated from time integrated concentrations of Table 5. This value is just above the annual 1 mSv ICRP (ICRP, 2007) reference level.

3.2. Ambient dose equivalent estimation

$H^*(10)$ have been calculated for i) immersion inside the radioactive cloud, ii) deposited radionuclides inside aircraft walls and iii) deposited

Table 6
Committed effective dose for a baby due to inhalation in the two scenarios selected, namely, a worst-case transoceanic flight and take-off and landing operations both during Fukushima accident.

Radionuclide	DPUI (mSv per Bq)	Time Integrated concentration inside cabin (Bq m^{-3} h)		E (mSv)	
		Transoceanic	Takeoff/ landing	Transoceanic	Takeoff/ landing
^{131}I particle	7.00E-05	3.70E+00	2.50E+03	2.6E-04	1.8E-01
^{131}I gas	1.50E-04	7.40E+00	5.00E+03	1.1E-03	8.0E-01
^{134}Cs	1.20E-05	3.70E-01	2.50E+02	4.4E-06	3.0E-03
^{137}Cs	1.00E-05	3.70E-01	2.50E+02	3.7E-06	3.0E-03
^{132}Te+^{132}I	5.00E-05	9.25E-02	2.50E+03	4.6E-06	1.3E-01
^{88}Kr	0.00E+00	3.70E+00	5.00E+03	0.0E+00	0.0E+00
^{133}Xe	0.00E+00	3.70E+02	5.00E+04	0.0E+00	0.0E+00
^{135}Xe	0.00E+00	3.70E+00	5.00E+03	0.0E+00	0.0E+00
		TOTAL		1.4E-03	1.1

Table 7
$H^*(10)$ due to immersion in an infinite cloud in the worst-case scenario for transoceanic and take-off operations.

Radionuclide	$H^*(10)$ (nSv h^{-1} per Bq m^{-3})	Time Integrated concentration (Bq m^{-3} h)		$H^*(10)$ (mSv)	
		Transoceanic	Takeoff/ landing	Transoceanic	Takeoff/ landing
^{131}I particle	4.90E-01	1.85E+00	2.50E+03	0.9E-06	1.2E-03
^{131}I gas	4.90E-01	3.70E+00	5.00E+03	1.8E-06	2.5E-03
^{134}Cs	2.50E+00	1.85E-01	2.50E+02	0.5E-06	0.6E-03
^{137}Cs	8.46E-01	1.85E-01	2.50E+02	0.2E-06	0.2E-03
^{132}I	3.80E+00	4.63E-02	2.50E+03	0.2E-06	9.5E-03
^{132}Te	3.71E-01	4.63E-02	2.50E+03	0.0E+00	0.9E-03
^{88}Kr	3.67E+00	1.85E+00	5.00E+03	6.8E-06	18.4E-03
^{133}Xe	6.24E-02	1.85E+02	5.00E+04	11.5 E−06	3.1E-03
^{135}Xe	4.28E-01	1.85E+00	5.00E+03	0.8E-06	2.1E-03
		TOTAL		22.7E-06	38.6E-03

particles outside aircraft walls, and for both scenarios, i.e., during the transoceanic flight and during take off and land operations.

3.2.1. Fictitious Cruise scenario- Transoceanic flight during Fukushima accident

3.2.1.1. Immersion inside the radioactive cloud. It is assumed that the passengers and crew are exposed for 10-h with no shielding due to the aircraft walls. The exposure is estimated based on percentages of time the snapshot of the FLEXPART simulations. The fluence rates are calculated using PENELOPE/penEasy code for a radioactive cloud size of 10-km x 10-km x 3-km. The $H^*(10)$ rates are estimated using equation (3), where A is the activity in the cloud in Bq, obtained from the average concentration for each radionuclide (Table 4) multiplied by the 300 km^3 volume of the radioactive cloud. In Table 7, the $H^*(10)$ rate per Bq m^{-3}, the corresponding time integrated concentration (Table 4), its contribution to $H^*(10)$ and the total $H^*(10)$ are shown. The calculated total $H^*(10)$ of 22.7 nSv is not significant and negligible compared to the dose due to inhalation.

3.2.1.2. Deposited radionuclides inside aircraft walls. Following, a simplified method to calculate the dose due to deposited radioactive particles inside on the wall of the aircraft is carried out for ^{137}Cs. First, it should be considered that the deposited particles on the walls will remain there unless a specific cleaning process is carried out. Furthermore, after an aircraft has flown inside a radioactive cloud and landed, a control of its contamination will be carried out. Therefore, in a conservative calculation, it can be assumed that the integrated deposition rate on the walls occurred at the beginning of the flight and during that flight time of 10-h the passengers and crew were irradiated.

The deposited activity rate can be calculated with the equation:

$$\dot{A}_{dep} = \left(2\frac{C}{C_o}\right) C_o v_{dep} \quad [4]$$

in Bq m^{-2} h, where.

C/C_o is the ratio of the concentration inside the aircraft to the concentration in the radioactive cloud and is obtaining by solving equation [1]. No retention of the filter is considered for calculations, so, C/C_o is 1. The factor 2 is included to take into account the double density inside the aircraft compared to outside, C_o is the concentration in the radioactive cloud in Bq m^{-3}, v_{dep} is the deposition velocity in m h^{-1} (a value of 0.02 m h^{-1} was estimated previously according to the work of Porstendörfer, 1994).

In order to calculate the accumulated deposited activity:

$$A_{dep} = \sum_{i=1}^{n} 2\, C_o(i) v_{dep} \Delta t_i \quad [5]$$

in Bq m^{-2}, where.

$C_o(i)$ is the concentration of the radionuclide in the cloud at time i in Bq m^{-3}.

Δt_i is the period of time with the concentration $C_o(i)$ in hours.

In order to calculate the external dose, it is assumed that the radionuclide is completely deposited at time zero. For instance, for ^{137}Cs, the time integrated concentration is 0.185 Bq m^{-3} h (Table 4). Therefore, using equation (5), the accumulated deposited activity on the walls is $7.4{\cdot}10^{-3}$ Bq m^{-2}.

The fluence distribution for deposited ^{137}Cs activity has been calculated using PENELOPE/penEasy for a cylindrical tube of 4-m diameter and 40-m length representing the A320 aircraft. The calculated conversion coefficient for ^{137}Cs is 1.67 nSv h^{-1} per kBq m^{-2}. Assuming a 10-h flight the total $H^*(10)$ is 1.2 10^{-4} nSv (1.67 nSv h^{-1} per kBq m^{-2} x $7.4{\cdot}10^{-6}$ kBq m^{-2} x10 h). Therefore, doses from the walls are not further considered in the analysis.

3.2.1.3. Deposited particles outside aircraft walls. Deposited particles on the outside walls of the aircraft are complicated to evaluate since the attached fraction of particles is not known. In any case, the $H^*(10)$ rate conversion factor per unit deposited activity will be lower than for the inside walls because of the wall attenuation. In order to calculate the outside deposited particles on the aircraft walls, an extremely conservative calculation can be carried out assuming that all particles where the aircraft passes through, when is inside the radioactive cloud, are deposited on the aircraft the wall. The traveling distance is assumed to be 8000 km with an equivalent concentration of 18.5 mBq m^{-3} for ^{137}Cs. Considering an aircraft diameter of 4 m, the volume the aircraft passes through is about 1.0 10^8 m^3. Therefore, assuming that all the activity in this volume is deposited on the aircraft walls, led to a maximum deposited activity of 1850 kBq. Then, assuming the aircraft as a cylinder of 4-m diameter and 40-m length, the activity per unit surface is about 3.7 kBq m^{-2}. Using the dose conversion coefficient 1.67 nSv h^{-1} per kBq m^{-2}, the total $H^*(10)$ for ^{137}Cs for this scenario assuming 10 h exposure is about 62 nSv. Therefore, the dose contribution from outside walls can also be neglected.

3.2.2. Take-off/landing scenario - Low altitude flight

3.2.2.1. Immersion inside the radioactive cloud. $H^*(10)$ rate is calculated in a similar way as for the transoceanic flight but using the corresponding time integrated concentrations. Table 7 shows that the external dose is about 40 μSv, which is considered not to be relevant from the radiological point of view under the current recommendations from the ICRP for the general public exposure.

3.2.2.2. Deposited radionuclides inside aircraft walls. Following the same procedure as for transoceanic flight the dose from ^{137}Cs is about $8.4{\cdot}10^{-2}$ nSv. Therefore, the total contribution from this source can be neglected.

3.2.2.3. Deposited particles outside aircraft walls. In this case the deposited particles on the outside aircraft walls are estimated according a flight within a radius of 100 km around the NPP. Therefore the volume of the flight is 1.3 10^6 m^3. The average activity during this flight period is 0.5 kBq m^{-3}. This led to a deposited activity of 6.4 10^2 kBq and an activity per unit area of 1.3 kBq m^{-2}. Using the dose conversion coefficient 1.67 nSv h^{-1} per kBq m^{-2}, the total $H^*(10)$ rate for ^{137}Cs in the worse scenario is about 20 nSv. Therefore, the dose contribution from outside walls can again be neglected.

4. Monitoring in aircrafts: is this the next step?

The installation of radiation detectors inside the cabin has three

objectives i) to estimate the dose ii) to provide information to pilots as well as others, on the ground in real time, to support decision, maybe included in the Aircraft Meteorological Data Relay (AMDAR) observing system (WMO, 2003) and iii) to provide data to be included in atmospheric transport models (ATM) in order to improve the simulation using data assimilation techniques.

Two types of detectors can be installed inside the cabin: i) air sampling monitors for radioactive gases and aerosol and ii) devices for monitoring the external dose rate. In the latter case, the use of spectrometric detectors using scintillators is recommended due to their large use in environmental surveillance, low response to cosmic radiation and the possibility to identify the radionuclides in the radioactive cloud. In the following the spectrometric option is explored because they can be installed in the aircraft easily than air sampling units. Furthermore, they are relatively light compared to iodine or aerosol monitors and easier to manage. They do not need pumps and filters and usually they are prepared to be used for relative long periods of time using batteries.

A spectrometric detector to be installed in an aircraft should be robust and not sensitive to vibrations. Furthermore, it should be pointed out that in case radioactive aerosols reach the cabin, the deposited particles on the surface of the detector itself could make a significant contribution to the measured spectra (Kessler et al., 2017) but not contribute to the dose to passengers and crew, and would thus produce an overestimation of the radioactive aerosol concentration in the cloud. It is recommended to cover the detector with a thin plastic film and change the film periodically in order to avoid the contribution of particles deposited on the surface of the monitor.Example of a detector that could be installed in an aircraft is a 3″ diameter x 12″ length NaI detector. The NaI crystal size of about 1.5 L (3″ diameter x 12” length) is considered one of the biggest portable spectrometric monitors. Furthermore, comparing it with the huge ones of 8 or 16 L is easier to be installed inside an aircraft.

The response of this detector due to a radioactive cloud of 10-km x 10-km x 3-km length is analysed. In order to calculate the response of the detector in the energy bin i, R_i in cps per kBqm^{-3}, the following expression is used:

$$R_i = \sum_{j=i}^{n} \phi_j p_{i,j} V \gamma \quad [6]$$

Where.

ϕ_j is the fluence per emitted photon in the cloud of energy j in cm^{-2}. The fluence is obtained using Monte Carlo (MC) simulations.

$p_{i,j}$ is the detector efficiency at energy bin i per unit fluence for an incident gamma flux of energy bin j, expressed in cm^2. For i = j, the $p_{j,j}$ values are the photo-peak efficiencies (ε_j). The detector efficiencies are calculated by MC simulations with parallel photon fluences perpendicular to the vertical axis of the monitor in 1/eV (for example 4.86 10^{-4} 1/eV for 660 keV). The surface of the parallel beam, S_f, is 232.26 cm^2 (3″x12″). The simulations are carried out with an energy bin of 1 keV. For example, ε_j for i = 660 keV is:

$$\varepsilon_{660} = MC_{output} \Delta E_{bin} S_f = 4.86\ 10^{-4} 10^3 232.26 = 112.9\ cm^2 \quad [7]$$

V is the volume of the radioactive cloud in m^3, in this case, the volume is 3 10^{11} m^3.

γ is the yield for the corresponding gamma decay of the radionuclide in s^{-1} Bq^{-1}.

In Table 8, the response of the detector located in the center of the radioactive cloud and at 6-km from the center of the cloud, i.e., 1-km distance from the border of the cloud for different radionuclides is shown. The response of the detector to the radioactive cloud will be mainly due to scattering photons. This effect can be seen in the calculated ratios of the photo-peak to total counts which are less than 1% when the aircraft is located 1-km far away of the cloud and about 10% when the aircraft is inside the cloud. In future studies, this effect could be used in order to know if the aircraft is inside or outside the radioactive cloud.

In order to complete the study of the 3″x12″ NaI detector response, simulated spectra have been calculated when the aircraft is flying at cruise altitude. In order to obtain a realistic spectrum in case of an accident a measurement campaign with an Embraer Legacy 600 aircraft has been carried out at 12 km altitude over the aerial space of Prague. These spectra are called background and their main contribution is due to the cosmic radiation. A typical 1 s measured spectrum is shown in Fig. 4 (blue line). A description of the cosmic radiation can be found elsewhere such as in the UNSCEAR 2008 report (UNSCEAR, 2008). Whereas at ground level the main cosmic contribution to the dose is the muon component (about 0.03 μSv h^{-1}), at cruise aircraft altitudes neutrons, electrons, positrons, photons and protons are the most significant contributors to the dose (about 4 μSv h^{-1}). However, it should be pointed out that scintillator detectors are mainly sensitive only to the photon component, which represents less than the 25% of the total dose at flight altitude (UNSCEAR, 2008).

The simulation has been carried out according to 1 Bq m^{-3} for ^{137}Cs and ^{134}Cs, 30 Bq m^{-3} for ^{131}I and 1 kBqm^{-3} for ^{133}Xe according to values for the flight over the ocean during the Fukushima accident.

The simulation for a 1 s spectrum is shown in Fig. 4. It can be seen that the most predominant peak is the one from ^{133}Xe. However, due to its low energy some attenuation is expected in a real situation since the walls of the aircraft have not been considered in the simulations. It can be noted that in the background spectrum, the pair production peak at 511 keV can be seen and could be used to re-calculate the energy calibration curve. The energy resolution according to the full width at half maximum (FWHM) was calculated using different radionuclide sources and following the expression suggested in Knoll (1998):

$$FWHM = 2.33\sqrt{E} \quad [8]$$

Where E is the energy in keV.

5. Conclusions for traffic management and recommendations for the aviation sector

The probability that a catastrophic nuclear accident similar to the Fukushima Dai-ichi accident would produce significant doses to the passengers and crew of an aircraft is very low based on the worst-case scenarios designed for this event. During the flight, at cruise altitude, the calculated doses are much lower than the reference value of 1 mSv for the public. During flights near the accident location the doses can come close to the reference levels. In this instance, network monitors on ground and close to the NPP location provide information on the radiological risk to decision makers in order to decide on recommendations due to the radiological incident. The exclusion zone could be extrapolated vertically, to determine a no-fly zone, as happened during the Fukushima accident, when the Japanese government declared an exclusion zone of 30 km radius around the NPP as a no-fly zone (IAEA, 2011). One of the most important complications to make any assessment is the lack of measurements other than at ground levels. A spectrometric detector installed in the aircraft can provide an estimation of the activity concentration in the radioactive cloud. This information can be useful to be assimilated in the atmospheric transport models in order to improve the simulations of the radioactive cloud dispersion in the atmosphere. Furthermore, this detector can provide the $H^*(10)$ rate to the passengers and crew can as well be useful to provide a rough estimate of the internal dose. However, surfaces, filters and other objects of the aircraft can become contaminated and a decontamination procedure and handling must be established after the aircraft lands. This contamination can be minimized if the aircraft has radioactive monitoring systems installed and the route is modified to avoid the radioactive cloud in combination with the atmospheric transport modeling tools and the agreed reference levels on potential risk that would provide useable charts for dispatchers and pilots.

Table 8
Response of a 3″x12″ NaI detector for different radionuclides in the center of the radioactive cloud and at 1 km distance.

E (keV)	Yield (s^{-1} per Bq)	ε_i (cm^2)	Fluence (cm^{-2} per history) Center/At 1 km	Photo-peak (cps per kBq m^{-3}) Center/At 1 km	Total (cps per kBq m^{-3}) Center/At 1 km	Ratio (%) Center/At 1 km
^{133}Xe						
81	0.37	211.7	4.23E-14/ 7.97E-19	9.94E+02/ 1.87E-02	6.19E+03/ 3.58E+00	16.1/ 0.5
^{135}Xe						
250	0.9	206	5.93E-14/ 1.43E-17	3.30E+03/ 7.95E-01	3.08E+04/ 1.37E+02	10.7/ 0.6
^{131}I						
365	0.812	137.2	6.77E-14/ 3.74E-17	2.26E+03/ 1.25E+00	3.03E+04/ 2.23E+02	7.5/ 0.6
^{137}Cs						
662	0.85	112.7	8.67E-14/ 1.66E-16	2.49E+03/ 4.77E+00	3.52E+04/ 5.64E+02	7.1/ 0.8
^{134}Cs						
569	0.154	126.5	8.11E-14/ 1.13E-16	4.74E+02/ 6.60E-01		
605	0.976	120.8	8.33E-14/ 1.32E-16	2.95E+03/ 4.67E+00		
796	0.85	97.6	9.45E-14/ 2.59E-16	2.35E+03/ 6.45E+00		
				5.77E+03/ 1.18E+01	8.29E+04/ 1.51E+03	7.0/ 0.8

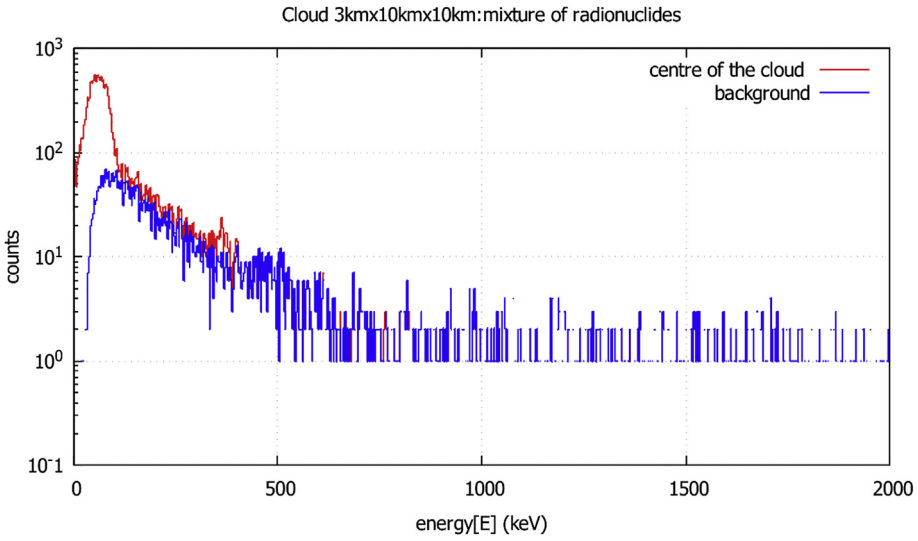

Fig. 4. Simulated spectra of the 3″x12″ NaI detector when the aircraft is in the center of the cloud for a mixture of radionuclides and concentrations obtained from simulation of the Fukushima accident.

It is important to stress that this work is a first step to be pursued further in the future and that it does not include any operational aspects. In particular, should the option of including monitoring devices in commercial aircrafts be realized, additional in depth discussions with the different stakeholders, manufacturers and policy makers should take place starting a lengthy process from concept to actual implementation and usage. It is also to be noted, that this very preliminary work does not include a full assessment of all the uncertainties existing, ranging from those related to the measurements, the dose simulations and the atmospheric transport modeling, being the latter one critical and of utmost importance since it links to the usually limited knowledge of the actual type and amount of radionuclides released into the atmosphere. Such uncertainties support once more the conservative approximation taken with focus on a worst-case scenario. In future work, an uncertainty range could be estimated, for example, by using ensemble modeling approaches both for the source term and the meteorological and atmospheric transport models used in addition to a more quantitative assessment of the uncertainties from the measurement side.

Lastly, although the doses estimated in this study are small, having proper estimate of the radioactive cloud either with atmospheric transport modeling, measurements or, ideally, a combination of both, would enable following the ALARA criteria and the pilot could reroute accordingly.

This work is seen as a starting point to potential follow-up activities that could comprise:

1. Further investigation based on a simulation scenario with a fictitious, but known emission, realistic flight tracks and with synthetic measurements at ground levels and the assumption that each aircraft would include a radiological spectrometric detector. The response of that fleet of detectors should then be simulated to identify what actual information they would provide in such an event and how this information could be used.
2. Study, based on 1, how the decision process could be improved through a) better information to decision makers. This should include a set of forecast charts at flight altitudes showing the amount of radioactivity and the definition of operational intervention levels, and b) inclusion of those measurement in simulation activities that would allow a better understanding of the extend and evolution of the radioactive cloud especially by aircraft measurements.
3. Last, but not least, investigation of the option for citizen science, taking into account the possibility of smartphones with embedded gamma dose rate monitors which would de facto translate in the order of hundreds of detectors in a plane.

Acknowledgements

The research leading to these results has received funding from the European Union's Horizon 2020 Research and Innovation Programme, under Grant Agreement no 723986. The research flight has been part of the research activities of the CRREAT (Research Center of Cosmic Rays and Radiation Events in the Atmosphere) project funded by the

European Structural and Investment Funds under the Operational Program Research, Development and Education (CZ.02.1.01/0.0/0.0/15_003/0000481.)

References

Ahmed, A.-R.A., 1979. Untersuchungen zur aerosol deposition an Oberflächen. Inaugural-Dissertation zur Erlanden des Doktorgrades der Naturwissenschaften der Justus-Liebig-Universität, Gissen.

EASA Safety Information Bulletin SIB 2011-4. available at: https://ad.easa.europa.

Grythe, H., Kristiansen, N.I., Groot Zwaaftink, C.D., Eckhardt, S., Ström, J., Tunved, P., Krejci, R., Stohl, A., 2017. A new aerosol wet removal scheme for the Lagrangian particle model FLEXPARTv10. Geosci. Model Dev. 10, 1447–1466. https://doi.org/10.5194/gmd-10-1447-2017.

Hiramaya, H., Matsumura, H., Namito, Y., sanami, T., 2015. Estimation of time history of 131I in air using NaI(Tl) detector pulse height distribution posts in Fukushima prefecture. Atom. Energy Soc. Jpn. 14 (No. 1), 1–11. https://doi.org/10.3327/taesj.J14.027.

Hubbell, J.H., Seltzer, S.M., 2004. Tables of X-Ray Mass Attenuation Coefficients and Mass Energy-Absorption Coefficients (Version 1.4). National Institute of Standards and Technology, Gaithersburg, MD Available at: http://physics.nist.gov/xaamdi.

IAEA Fukushima Nuclear Accident Update Log, 2011. Updates of 15 March 2011, available at: https://www.iaea.org/newscenter/news/fukushima-nuclear-accident-update-log-21.

ICAO, 2016a. Annex3-Meteorological services for international air navigation – Part I and II. available at: https://store.icao.int/annex-3-meteorological-services-for-international-air-navigation-english-printed.html July 2016a.

ICAO, 2016b. Report of the Second Meeting of the Meteorology Panel. (MEPT 2016), Montreal 17-21 October 2016. Available at: https://www.icao.int/airnavigation/METP/Panel%20Meetings/METP2%20Final%20report.pdf.

ICRP, 1994. Human respiratory tract model for radiological protection. ICRP Publication 66. Ann. ICRP 24 (1–3).

ICRP, 1995. Age-dependent doses to members of the public from intake of radionuclides - Part 4 inhalation dose coefficients. ICRP Publication 71. Ann. ICRP 25 (3–4).

ICRP, 2007. The 2007 recommendations of the international commission on radiological protection. ICRP Publication 103. Ann. ICRP 37 (2–4).

ISO 4037-3 INTERNATIONAL ORGANIZATION FOR STANDARDIZATION, 1999. X and Gamma Reference Radiation for Calibrating Dosemeters and Dose Rate Meters and for Determining Their Response as Function of Photon Energy. Part 3: Calibration of Area and Personal Dosemeters and the Measurement of Their Response as a Function of Energy and Angle of Incidence. vol. 4037 ISO 3.

IRSN, 2011. Information Report, 22 March 2011. available at: https://www.irsn.fr/EN/newsroom/News/Documents/IRSN_fukushima-radioactivity-released-assessment-EN.pdf.

Kristiansen, N.I., Stohl, A., Olivié, D.J.L., Croft, B., Søvde, O.A., Klein, H., Christoudias, T., Kunkel, D., Leadbetter, S.J., Lee, Y.H., Zhang, K., Tsigaridis, K., Bergman, T., Evangeliou, N., Wang, H., Ma, P.-L., Easter, R.C., Rasch, P.J., Liu, X., Pitari, G., Di Genova, G., Zhao, S.Y., Balkanski, Y., Bauer, S.E., Faluvegi, G.S., Kokkola, H., Martin, R.V., Pierce, J.R., Schulz, M., Shindell, D., Tost, H., Zhang, H., 2016. Evaluation of observed and modelled aerosol lifetimes using radioactive tracers of opportunity and an ensemble of 19 global models. Atmos. Chem. Phys. 16, 3525–3561. https://doi.org/10.5194/acp-16-3525-2016.

Kessler, P., Camp, A., Dombrowski, H., Neumaier, S., Röttger, A., Vargas, A., 2017. Influence of radon progeny on dose rate measurements studied at PTB's radon reference chamber. Radiation Protection Dosimetry. Available on line. https://doi.org/10.1093/rpd/ncx059.

Knoll, G.F., 1989. Radiation Detection and Measurement, second ed. John Wiley & Sons, Inc, New York, NY,USA.

Masson, et al., 2011. Tracking of airborne radionuclides from the damaged Fukushima dai-ichi nuclear reactors by european networks. Environ. Sci. Technol. 45 (18), 7670–7677 2011.

Porstendörfer, J., 1994. Properties and behaviour of radon and thoron and their decay products in the air. J. Aerosol Sci. 25 (No. 2), 219–263.

Salvat, F., Fernández-Varea, J.M., Sempau, J., 2011. PENELOPE-2011: A Code System for Monte Carlo Simulation of Electron and Photon Transport (No. NEA/NSC/DOC(2011)5). Nuclear Energy Agency. Workshop Proceedings. Barcelona.

Sempau, J., Badal, A., Brualla, L., 2011. A PENELOPE-based system for the automated Monte Carlo simulation of clinacs and voxelized geometries—application to far-from-axis fields. Med. Phys. 38 (11).

Slinn, W.G.N., 1982. Predictions for particle deposition to vegetative canopies. Atmos. Environ. 16, 1785–1794. https://doi.org/10.1016/0004-6981(82)90271-2.

Stohl, A., Forster, C., Frank, A., Seibert, P., Wotawa, G., 2005. Technical Note: the Lagrangian particle dispersion model FLEXPART version 6.2. Atmos. Chem. Phys. 5, 2461–2474.

Stohl, A., Seibert, P., Wotawa, G., Arnold, D., Burkhart, J.F., Eckhardt, S., Tapia, C., Vargas, A., Yasunari, T.J., 2012. Xenon-133 and caesium-137 releases into the atmosphere from the Fukushima Dai-ichi nuclear power plant: determination of the source term, atmospheric dispersion, and deposition. Atmos. Chem. Phys. 12, 2313–2343. https://doi.org/10.5194/acp-12-2313-2012.

UNSCEAR, 2008. Report. *Sources, Effects and Risks of Ionizing Radiation.* Volume I, Scientific Annex B: Exposures of the Public and the Workers from Various Sources of Radiation.

UNSCEAR, 2013. Report. *Sources, Effects and Risks of Ionizing Radiation.* Volume I, Scientific Annex A: Levels and Effects of Radiation Exposure Due to the Nuclear Accident after the 2011 Great East-Japan Earthquake and Tsunami.

WMO, 2003. Aircraft Meteorological Data Relay (AMDAR) Reference Manual. Secretariat of the World Meteorological Organization, Geneva, Switzerland.